Computers & Geosciences 192 (2024) 105709

Contents lists available at ScienceDirect

Computers and Geosciences

journal homepage: www.elsevier.com/locate/cageo

Combining deep neural network and spatio-temporal clustering to automatically assess rockburst and seismic hazard – Case study from Marcel coal mine in Upper Silesian Basin, Poland

Adam Lurka *

Central Mining Institute (GIG), Laboratory of Mining Geophysics, Katowice, Poland

ARTICLE INFO

Keywords:
Deep learing
Convolutional neural network
Cluster
Mining tremor
Seismic hazard
Rockburst
Categorical data analysis

ABSTRACT

Mine induced seismic events are a major safety concern in mining and require careful monitoring and management to reduce their effects. Therefore, an essential step in assessing seismic and rock burst hazards is the analysis of mine seismicity. Recently, deep neural networks have been used to automatically determine seismic wave arrival times, surpassing human performance and allowing their use in seismic data analysis such as seismic event location and seismic energy calculation. In order to properly automate the rockburst and seismic hazard assessment deep neural network phase picker and a spatio-temporal clustering method were utilized. Seismic and rockburst hazards were statistically quantified using two-way contingency tables for two categorical variables: seismic energy level of mine tremors and number of clusters. Correlations between several spatio-temporal clusters and a statistical association between two categorical variables: seismic energy level and cluster number indicate an increase of seismic hazard in the Marcel hard coal mine in Poland. A new automated tool has been elaborated to automatically identify high-stress areas in mines in the form of spatio-temporal clusters.

1. Introduction

Mining induced seismicity refers to earthquakes that are caused by mining activities, specifically activities like extracting coal and ore in underground mines. These seismic events can cause significant damage to the mine and surrounding areas resulting in rock-bursts, which are sudden, violent releases of energy within the mine that can cause major structural damage, (Bai et al., 2022; Niu et al., 2022; Zhou et al., 2021; Cai et al., 2019; Gong et al., 2019). The occurrence of mining induced seismicity is a major safety concern in the mining industry and requires careful monitoring and management to minimize its impact, (Shuai et al., 2023). Moreover, to assess the seismic and rockburst hazard, it is important to analyze the seismicity caused by mining, (Cao et al., 2020; Mutke et al., 2015; Orlecka-Sikora et al., 2012; Riemer and Durrheim, 2012; Kwiatek et al., 2010).

One of the most time consuming and indispensable steps in the analysis of mining seismic events is the determination of arrival times of seismic waves. This step is most often performed manually because the existing automatic algorithms provides very erroneous results and further analysis of mining seismicity such as location and seismic energy calculation requires high quality arrival times of seismic waves. Only recently have deep neural networks begun to be used for automatic determination of arrival times of seismic waves, outperforming human performance, (Johnson et al., 2021; Zhu et al., 2021; Mousavi et al., 2020; Chai et al., 2020; Wang et al., 2019; Zhu et al., 2019; Ross et al., 2018) and allowing their use in seismic data analysis such as seismic event location and seismic energy calculation.

Deep neural networks (DNNs) have been increasingly used in seismology to improve the accuracy of seismic data processing, event detection, classification, fault recognition and earthquake forecasting, (Liu and Chen, 2023; Mao et al., 2023; Xu et al., 2023; Ding et al., 2022; Ma et al., 2022; Niu et al., 2022; Pu, et al., 2020, 2022; Wang and Tang, 2022; Woollam et al., 2022; Xu et al., 2022; Zou et al., 2022; An et al., 2021; Duan et al., 2021; Wang et al., 2021; Wilkins et al., 2020; Geng et al., 2019), as well as in geotechnical underground engineering (Zhang and Phoon, 2022; He et al., 2019; Sun et al., 2019). DNNs are a type of artificial neural network that can learn complex features and relationships from data through multiple layers of nonlinear transformations. DNNs have been applied to various tasks in seismology, including seismic waveform processing to denoise and filter seismic waveforms, seismic event detection and classification to detect and classify different types of seismic events, such as earthquakes, explosions, and tremors.

* Główny Instytut Górnictwa, 40-166, Katowice, plac Gwarków 1, Poland.
E-mail address: alurka@gig.eu.

https://doi.org/10.1016/j.cageo.2024.105709
Received 22 November 2023; Received in revised form 8 May 2024; Accepted 29 August 2024
Available online 30 August 2024

DNNs can also be used to distinguish between natural and induced seismicity, and to identify seismic events that are associated with specific geological structures and processes. DNNs can be used to predict the likelihood and magnitude of future earthquakes and to identify seismic precursors, which are signals that precede a major earthquake and may provide early warning. DNNs have several advantages over traditional methods in seismology, including their ability to handle large volumes of data, learn complex patterns and relationships, and adapt to changing conditions. However, DNNs also require large amounts of data and computing resources, and their results can be difficult to interpret. Therefore, it is important to carefully validate and evaluate the performance of DNN models in seismology.

In mining seismology, clustering methods are used to identify patterns of seismic activity that may be related to mining operations. These methods can help identify regions of the mine that are at risk of seismic activity, and can inform decisions about mine design, blasting practices, and other safety measures, (Liu et al., 2023). There are various methods used for clustering mining seismic events. These methods are used to group mining earthquakes that occur closely in time and space. Some common clustering methods are as follows. The hierarchical clustering method is commonly used in seismicity analysis, including the study of seismic events in underground mines. It involves creating a dendrogram, which is a tree-like structure that shows the relationship between seismic events based on their similarity in space and time, (Lurka, 2021; Hudyma, 2008). K-means clustering is a statistical method that groups mining tremors based on their similarity in space. The method involves selecting a number of clusters and assigning each mining earthquake to a cluster based on its proximity to the cluster centroid, (Meyer et al., 2019; Leśniak and Isakow, 2009). Density-based clustering involves identifying areas of high seismicity density and grouping seismic events that occur within these areas, (Woodward et al., 2018).

The seismicity observed in underground mines is indeed influenced by various factors, including faults, dikes, pillars, rock characteristic, and spatial distribution of mine workings. In underground hard coal mines, a continuous cloud of seismicity often arises from mining-induced seismic events, (Wang et al., 2015). To analyze and understand such continuous seismicity, the spatiotemporal hierarchical clustering method proposed by Lurka (2021) can be effectively applied. This method involves grouping seismic events based on their spatial and temporal characteristics, allowing identification of patterns and relationships within the seismic data. The spatiotemporal hierarchical clustering method considers both the locations and timings of seismic events to identify clusters or groups of events that are closely related in space and time. This approach is particularly useful for longwall mining systems where a continuous cloud of seismicity is observed.

We propose in this study a novel algorithm that utilizes a deep neural network phase picker and a spatio-temporal clustering method to automate the assessment of rockburst and seismic hazard in the Marcel hard coal mine in Poland. The seismic and rockburst hazard is quantified statistically by utilizing two way contingency tables for two categorical variables: seismic energy level of mining tremors and cluster number. Thus, we have developed a new tool that enables automatic identification of high-stress areas in mines prone to high energy seismic activity. The novelty of our approach is twofold. First, categorical data analysis was used for the first time to assess seismic and rockburst hazard. Secondly, a heuristic algorithm was proposed that automates the seismic and rockburst hazard assessment process using deep learning, spatio-temporal clustering and categorical data analysis.

2. Materials and methods

We have analyzed in this study the seismic data from the Marcel coal mine, Upper Silesia, Poland in the area of the coal panel C-4/505, Fig. 1. Our experiment involved application of several consecutive methods: the deep convolutional neural PhaseNet model, (Zhu et al., 2019), seismic event location and seismic energy calculation, hierarchical cluster analysis with spatio-temporal metric, (Lurka, 2021) and categorical data analysis, (Agresti, 2012). Therefore, we have designed a workflow which takes advantage of these methods and show the interrelations between them, Fig. 2. The analyzed area, seismic data and each of the utilized methods are shortly described in the following paragraphs.

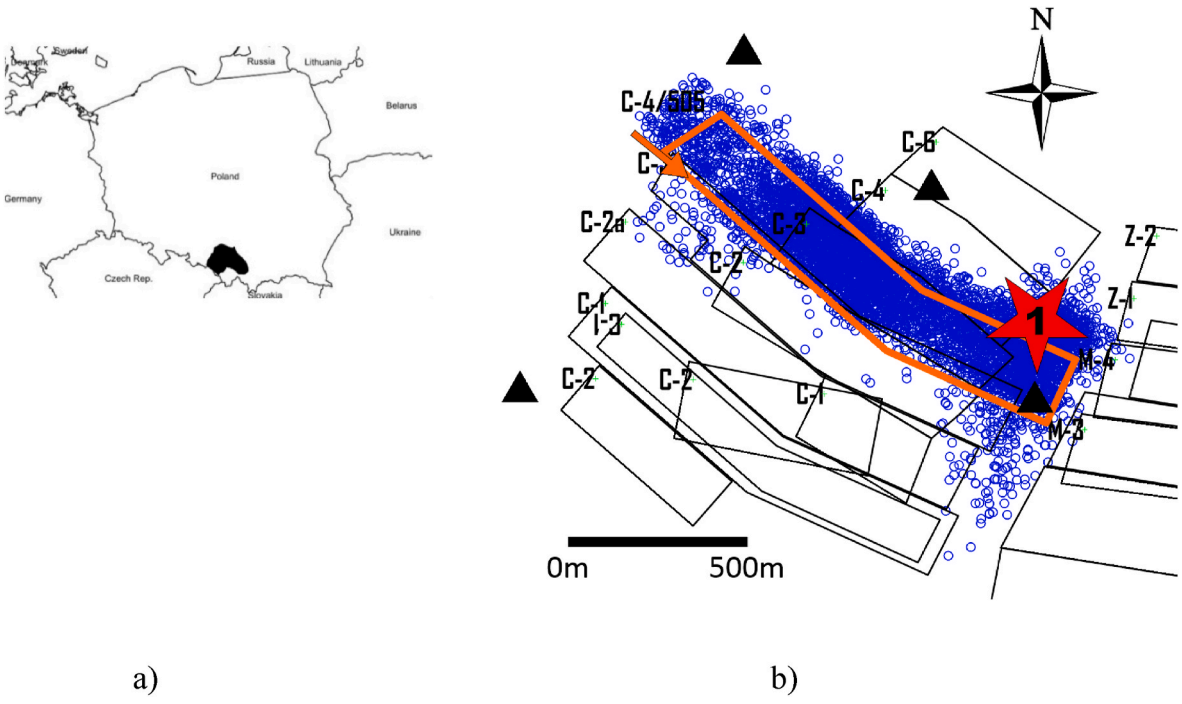

Fig. 1. a) Marcel hard coal mine in Upper Silesia, Poland is the most seismically active mining site in Europe; shown as the black area. b) Area of the coal panel C-4/505 in the Marcel coal mine. Recorded seismicity shown as blue circles and seismic stations as black triangles; rockburst marked as large red star; red arrow denotes coal face direction.

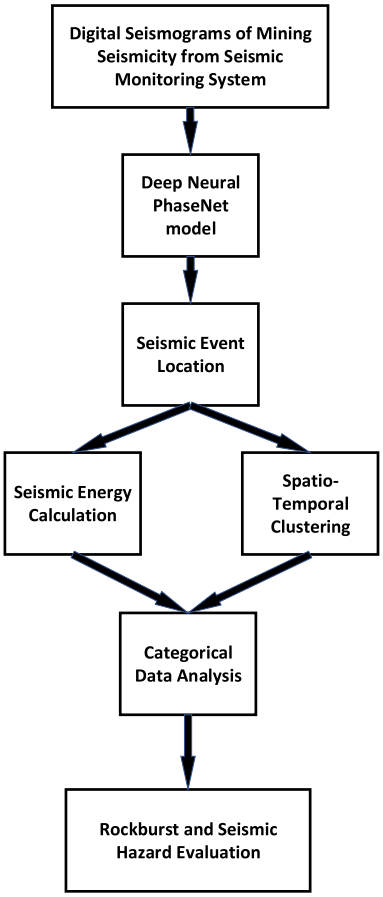

Fig. 2. A flowchart of automatic seismic and rockburst hazard assessment using a deep neural network model, spatio-temporal clustering and categorical data analysis.

2.1. Materials

The SOS seismic monitoring system was installed in the Marcel coal mine in Upper Silesia, Poland, at the beginning of 2000 consisting of 20 uniaxial velocity sensors with a natural frequency of 1Hz. The seismic sensors are located at the depth between 600 and 1000 m below the surface encompassing roughly the area 6 km in NW direction by 7 km in SN direction. The seismic network is centered around safety pillar where analyzed coal panel C-4/505 is located, Fig. 1b.

Four seismic stations were strategically positioned near the coal panel C-4/505, as illustrated in Fig. 1b. Additionally, sixteen other stations were placed at distances ranging from 2 to 6 km apart. The seismic event locations were determined by analyzing the first arrivals of the seismic longitudinal P wave. This process involved minimizing the arrival time residuals using the L1 norm and the Simplex iterative algorithm, as described by Prugger and Gendzwill (1988) and Press et al. (2007). To facilitate the location procedure, a uniform velocity model equal to 4050 m/s was utilized. This model was derived from underground blasting. The estimated location error of mining tremors varied from 10 to 30 m for XY coordinates and from 110 to 180 m for vertical Z coordinate. The formula we used for quantifying the location errors of mining-induced seismicity involved calculating the uncertainty in the measured coordinates X, Y and Z of a seismic event in the form of covariance matrix and taking the square roots of diagonal elements as standard error estimates of the corresponding coordinates, Thurber and Engdahl (2000). It is important to note that the accuracy of the seismic event locations depended on the several factors: network geometry, velocity model inaccuracies, signal to noise ratio and number of P wave onset times. For mining-related tremors, the locations were determined based on the onset times of the seismic P wave, which were picked at a minimum six seismic stations.

The underground microseismic system in the Marcel mine is operating continuously with a sampling rate of 500 samples per second, and its internal clock is synchronized by GPS with very high accuracy.

We have analyzed the data set encompassing the foreshock and aftershock sequence of the seismic event with the highest observed energy E = $2*10^7$[J] (magnitude M = 2.9) that occurred on February 8, 2019 and caused rockburst, Fig. 1b. The occurrence of the highest observed energy mining tremor serves as a valuable reference point for evaluating the stress changes both in space and time.

The preprocessing of seismic data before analysis is a crucial step in improving data quality and preparation for other tasks, such as locating seismic events and calculating seismic energy. We conducted noise reduction as the procedure to distinguish seismic signals from unwanted noise not related to any mining induced seismic events. To eliminate noisy data, we used a Butterworth bandpass filter in the frequency range from 1 Hz to 200 Hz.

Throughout the analyzed timeframe, a total of 5544 mining tremors were documented, out of which 2551 tremors exhibited energies ranging from 10^2[J]-10^3[J] (magnitudes 0.1–0.6), 2359 tremors with energies 10^3[J]-10^4[J] (magnitudes 0.6–1.2), 523 tremors with energies 10^4[J]-10^5[J] (magnitudes 1.2–1.7), 95 tremors with energies 10^5[J]-10^6[J] (magnitudes 1.7–2.2), 15 tremors with energies 10^6 [J]-10^7[J] (magnitudes 2.2–2.7) and one tremor having energy E = $2*10^7$[J] (magnitude M = 2.9), Fig. 3. The spatial distribution of microseismic events and recorded rockburst of Marcel mine are shown in Fig. 1b.

2.2. Methods

2.2.1. Automatic determination of the arrival times of seismic P-waves with the use of the deep neural network model PhaseNet

PhaseNet is a deep learning model developed for the automatic detection and picking of seismic phases, which are the arrival times of different types of seismic waves that are produced during an earthquake. These arrival times can be used to estimate the earthquake's location and magnitude. PhaseNet was developed by the seismology team at the Stanford University, Zhu& Beroza (2019), and it uses a deep convolutional neural network (CNN) architecture to analyze the raw seismic data and predict the arrival times of different seismic phases. The model

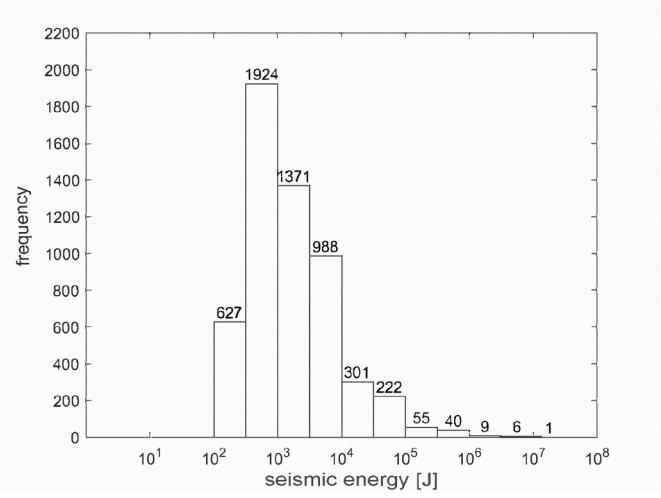

Fig. 3. A histogram depicting the seismic energies of mining tremors observed in Marcel mine during the period from November 1, 2017, to January 30, 2021. The dataset consisted of a total of 5544 recorded seismic events. The horizontal axis represents the seismic energy intervals measured in joules, while the vertical axis represents the number of seismic events falling within each energy interval.

was trained on a large dataset of about 1 million seismograms, which are recordings of ground motion produced by earthquakes, and it was able to achieve high accuracy in detecting seismic phases. The main advantage of PhaseNet is that it can accurately detect seismic phases even in noisy data, which is a common problem in seismology. This makes it a very valuable tool for seismicity monitoring and early warning systems.

The architecture of PhaseNet is based on U-Net model, (Ronnenberger et al., 2015) and the inputs the seismograms of recorded seismic events. The output of PhaseNet deep neural network is the probabilities of P and S wave onset times, but we have used P wave arrivals only due to the fact that S wave arrivals can be overlapped with other types of wave such as seismic scattered or coda waves. Therefore S wave onset times have inherently larger errors and are much more difficult to determine by automatic methods, (Zhu et al., 2019). The input seismic data pass through the down sampling process consisting of several convolution and rectified linear functions and up sampling process consisting of several deconvolution and rectified linear functions, (Zhu et al., 2019), which has been symbolically shown in Fig. 4.

2.2.2. Seismic event location and seismic energy calculation of mining tremors

After automatic determination of the arrival time of seismic P-waves utilizing the deep neural network model we have performed the location and seismic energy calculation of the analyzed mining induced seismicity.

2.2.2.1. Mining tremors location procedure. The location of a mining tremor is determined by analyzing arrival times of seismic P-waves. Location methods based on the arrivals times are closely related to the problem of minima determination of the function of several variables called objective function. We have utilized the time difference between the measured and theoretical arrival time of the seismic longitudinal P-wave and the L1 norm of the objective function, (Prugger&Gendzwill, 1988):

$$F(x_0, y_0, z_0, t_0) = \sum_{i=1}^{n} \left| t_i - t_0 - \frac{\sqrt{(x_0 - x_i)^2 + (y_0 - y_i)^2 + (z_0 - z_i)^2}}{V_P} \right| \tag{1}$$

where:

x_0,y_0,z_0 – the unknown seismic event coordinates [m],

t_0 – the unknown origin time of the seismic event [s],

x_i,y_i,z_i - coordinates of the seismic station no. "i"[m[],

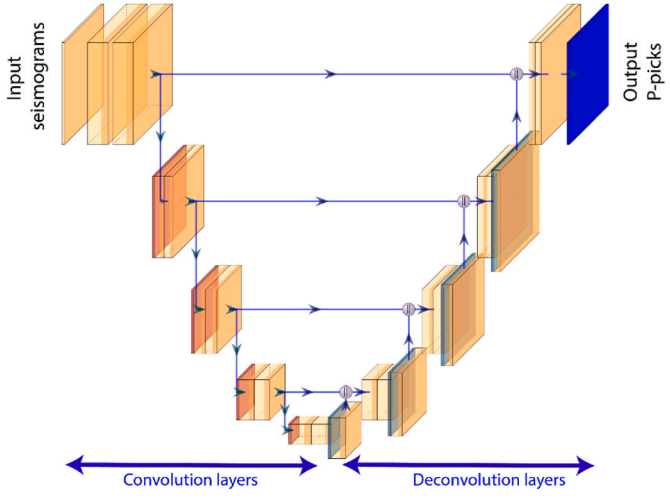

Fig. 4. The outline of the Convolutional Deep Neural Network PhaseNet architecture used in the analysis of the recorded seismograms for mining seismic events in Marcel mine. See Zhu et al. (2019) for more details.

n – total number of seismic stations,

t_i – arrival time of seismic P wave at the station number "i", determined by utilizing the deep neural network model PhaseNet [s]

V_P – P wave velocity model of the rock mass, assumed constant and equal to 4050 m/s determined from blast seismograms[m/s].

The objective function is minimized using Simplex iterative method, which update the location estimate iteratively until a minimum is reached, (Prugger&Gendzwill, 1988).

2.2.3. Seismic energy calculation of mining tremors

We have used ground motion velocity seismograms of mining induced seismicity to calculate the radiated energy of seismic P and S waves and then used its sum as the estimate of total radiated seismic energy of mining tremor. To obtain the seismic energy of S waves we first calculated the arrival times of seismic S wave at each seismic station. The method we have used is based on time integration of the squared ground velocity seismograms corrected for attenuation function, (Kanamori et al., 1993):

$$E_{P(S)} = 4\pi r^2 [r_0 q(r_0)/rq(r)]^2 \rho_0 \beta_{P(S)} \int v^2(t) dt \tag{2}$$

where:

ρ_0- density of the medium [kg/m^3],

$\beta_{P(S)}$- seismic P(S) wave velocity of the medium [m/s],

r – distance to the selected seismic station [m],

r_0 - distance to the focal sphere [m],

$q(r) = \frac{\exp(-\alpha r)}{r}$- attenuation function [1/m],

α- attenuation coefficient equal to 0.002 both for P and S waves [1/m].

2.2.4. Hierarchical clustering of mining seismicity

We have applied the agglomerative hierarchical clustering approach to perform spatio-temporal clustering on the mining seismic events recorded at the Marcel coal mine, shown in Fig. 1b. This clustering method is widely recognized and extensively used in various applications, (Lurka, 2021; Jain et al., 1999). The clustering procedure commences with a set of clusters, each initially composed of a single seismic event. As the procedure progresses, these clusters are gradually merged together, forming a hierarchical structure of clusters. This structure is commonly represented as a dendrogram, (Aggarwal&Reddy, 2014).

In the context of mining tremors, spatial (X,Y) and temporal (T) coordinates were introduced. These coordinates are used to describe the location and timing of seismic events within the mining area. The spatial coordinates refer to the physical position of the seismic events in the mining region, typically represented using Cartesian coordinates. On the other hand, the temporal coordinates refer to the time at which each seismic event occurs, usually represented as a timestamp or time interval. By incorporating both spatial and temporal coordinates, a comprehensive understanding of the distribution and timing of mining-induced seismicity can be obtained. We have omitted the vertical Z coordinate from our analysis due to large location errors of this component what would cause problems with obtaining reliable clustering results.

In order to examine mining seismicity comprehensively, considering both spatial and temporal aspects, we employ the following metric representing distance between two points in space and time, (Lurka, 2021):

$$\left\| p_i - q_j \right\|^2 = \left(p_{ix} - q_{jx} \right)^2 + \left(p_{iy} - q_{jy} \right)^2 + c^2 \left(p_{it} - q_{jt} \right)^2 \tag{3}$$

where:

$p_i = \left(p_{ix}, p_{iy}, p_{it} \right)$- spatio-temporal coordinates of mining seismic event number "i",

$q_j = \left(q_{jx}, q_{jy}, q_{jt} \right)$- spatio-temporal coordinates of mining seismic

event number "j",

$$c^2 = \frac{V(X) + V(Y)}{V(T)} \tag{4}$$

V(X), V(Y), V(T) – variances of the analyzed coordinates,

$\left\|p_i - q_j\right\|^2$ - the distance between two seismic events with coordinates p_i and q_j respectively.

2.2.5. Categorical data analysis of recorded seismicity

Categorical data analysis is a statistical method used to analyze data that is nominal or ordinal in nature, meaning it consists of categories or groups rather than numerical values. If the response and explanatory statistical variables are both categorical then the common approach is the construction of contingency tables, (Agresti, 2012). Two way contingency tables are often used in social science research, but can also be applied in other fields such as medicine, epidemiology, and engineering. A contingency table, also known as a cross-tabulation table or a two-way table, displays the frequency distribution of two categorical variables. Each variable is displayed as a row or column in the table, and the intersection of the row and column represents the frequency of cases that have both values.

In mining sciences and in particular in seismology, categorical data analysis can be used to analyze seismic data that is classified into different categories, such as earthquake magnitude, seismic energy, earthquake type, seismic intensity, or earthquake location. One common application of categorical data analysis in seismology is the study of earthquake magnitude distributions. Earthquake magnitudes or seismic energies can be typically classified into different categories, such as "small" "moderate" or "large". In such cases categorical data analysis can be used to examine the frequency of seismic events in each category. We have adopted this approach in our analysis of mining seismic data from Marcel coal mine i.e. the classification of mining seismic events into categories based on their energy.

Based on contingency tables with N rows and M columns we have calculated the chi-square statistics, which measures the independence of two categorical variables according to the following formula:

$$\chi^2 = \sum_{i=1}^{N} \sum_{j=1}^{M} \frac{\left(n_{ij} - \mu_{ij}\right)^2}{\mu_{ij}} \tag{5}$$

where:

χ^2– Pearson chi-squared statistic of the contingency table

n_{ij} – observed frequency of row number "i" and column number "j" in contingency table

μ_{ij} – estimated expected frequency of row number "i" and column number "j" in contingency table

The statistical test utilizing chi-square statistics allowed us to answer the question if there is any association between two categorical variables. The smaller the p-value of chi-square test the stronger the evidence of the association. However, to obtain a measure of how strong is the association between two categorical variables we have calculated two coefficients:

the contingency coefficient

$$C = \sqrt{\frac{\chi^2}{\chi^2 + NO}} \tag{6}$$

and the Cramer's V coefficient

$$V = \sqrt{\frac{\chi^2}{NO(N-1)}} \tag{7}$$

where:

NO –total number of observations.

The disadvantage of the C contingency coefficient is that it does not reach a maximum of 1.0 and therefore cannot be used to compare associations in different contingency tables. The Cramer V coefficient varies from 0, corresponding to no association between categorical variables, to 1, corresponding to complete association.

Contingency tables can also be used for understanding the relationship between two categorical variables, and help identify patterns or trends in our seismic data. To achieve this we have utilized the standardized residuals for cell in row "i" and column "j" of chi-square statistics:

$$e_{ij} = \frac{\left(n_{ij} - \mu_{ij}\right)^2}{\mu_{ij}} \tag{8}$$

The standardized residuals allowed us to highlight those cells in contingency tables that are more likely or less likely to occur than expected values under the independence assumption.

3. Results and discussion

Before we discuss the results, it is necessary to explain what is meant by seismic hazard and what is meant by rockburst hazard. In order to define these two concepts, it is first necessary to provide the definitions of mining-induced seismic event and rockburst.

A mining-induced seismic event refers to an earthquake that is directly caused by mining operations. These seismic events are typically a result of the stress fields changes in the rockmass due to the excavation which can activate existing faults, create new fractures. In cases where mining seismic event cause damage to underground workings, the seismic event is referred to as rockburst.

A seismic hazard refers to the probability or likelihood of an area being affected by seismic activity. It encompasses the potential ground shaking intensity, occurrence frequency and seismic energy distribution. This assessment helps in preparing management plans that can withstand or minimize potential damages caused by mining induced seismicity. A rockburst hazard refers to the potential risk of experiencing a rockburst in underground mining. This hazard is characterized by the likelihood of sudden and violent ejections of rock from the walls, roof, or floor of an excavation due to high stress concentrations in the rock. It follows that rock burst hazard is a very small subset of seismic hazard.

The presented discussion of the results includes a combined analysis of seismic and rockburst hazards based on the heuristic algorithm presented in the previous sections. This algorithm should be treated as a completely new indicator assessing seismic hazard based on categorical data analysis, having no equivalents among other methods assessing seismic and rockburst hazards. Therefore, it cannot be compared with other seismic hazard indicators.

3.1. Deep learning PhaseNet model analysis

According to the workflow in Fig. 2, in the first step, we have analyzed around one hundred thousand velocity seismograms recorded during our seismic monitoring campaign in Marcel coal mine as time series inputs to the PhaseNet deep neural network model, (Zhu et al., 2019). The duration of each of the analyzed velocity seismograms was about 13 s with sampling rate 0.002 miliseconds, Figs. 5–7. Originally the inputs of the PhaseNet model are three-components seismograms of recorded seismic events and outputs are probability distributions of P wave onset times, (Zhu et al., 2019). In our case the seismic monitoring system installed in the Marcel mine consisted of uniaxial sensors. Therefore we used three identical copies of one component seismograms recorded by these uniaxial sensors because three inputs to the PhaseNet model were required. Additionally, we used around 10% of the seismograms with manually picked P wave onset times to retrain the PhaseNet model and obtain better quality of the results. After retraining the PhaseNet model we have not found any improvement in the quality of

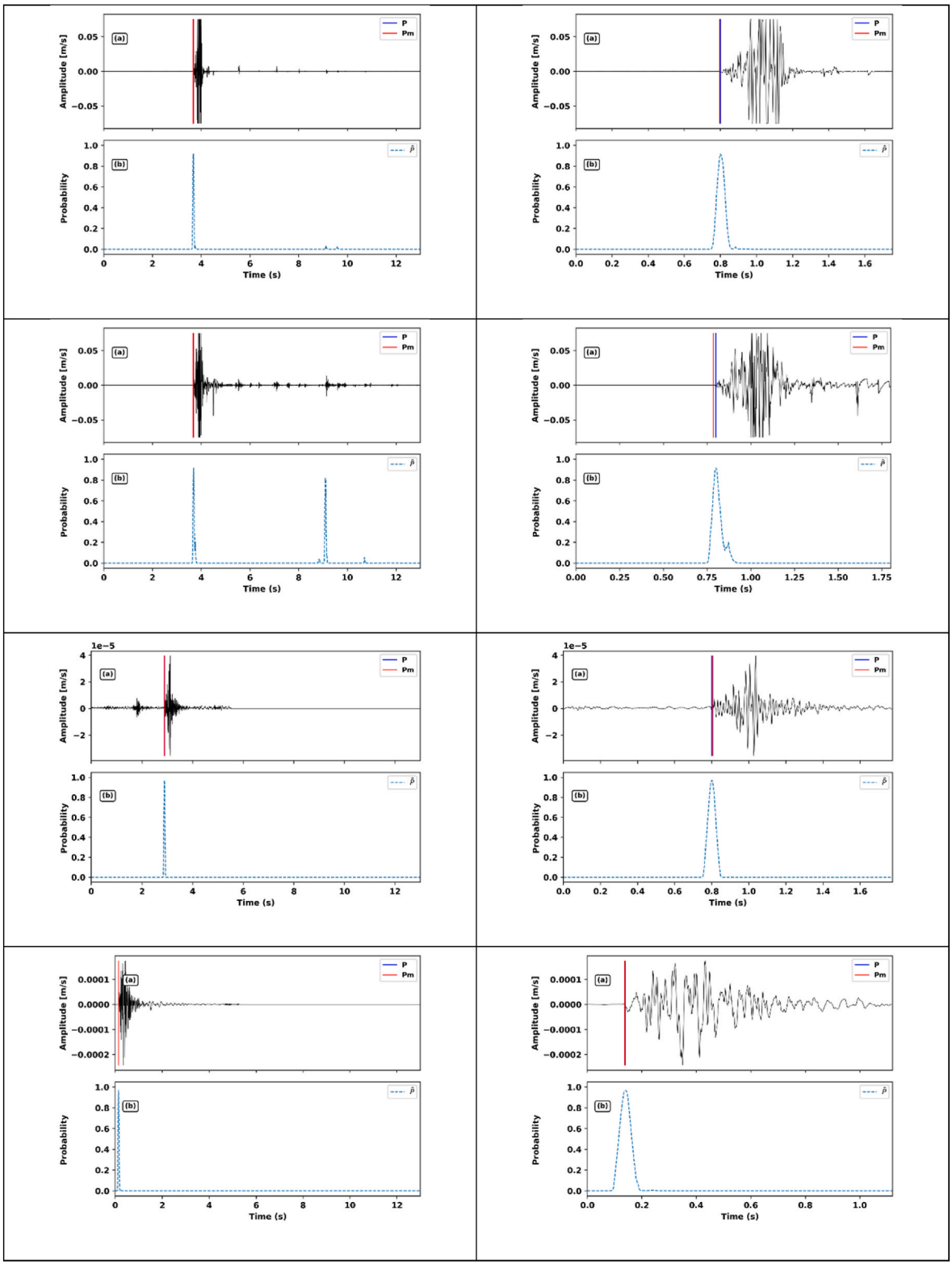

Fig. 5. Examples of picks of seismic P wave onset times in the analyzed data set with very small differences between manual picks determined by an expert (Pm) and picks determined by Deep Convolutional Neural Network PhaseNet (P). Left: seismograms shown in a long time window; Right: seismograms shown in a short time window.

the P wave picks determination compared with the original PhaseNet model results, most probably due to the fact that original PhaseNet model, trained on around one million velocity seismograms collected over a period of about 30 years, determined P wave onset times with very high accuracy outperforming in many cases P wave onset times obtained by human expert, Figs. 5–7. The analysis and determination of P wave onset times with the use of PhaseNet model on 100000 velocity seismograms took less than 10 min on regular PC computer, whereas the thorough analysis of the same number of velocity seismograms by experienced human expert would take a couple of months, clearly

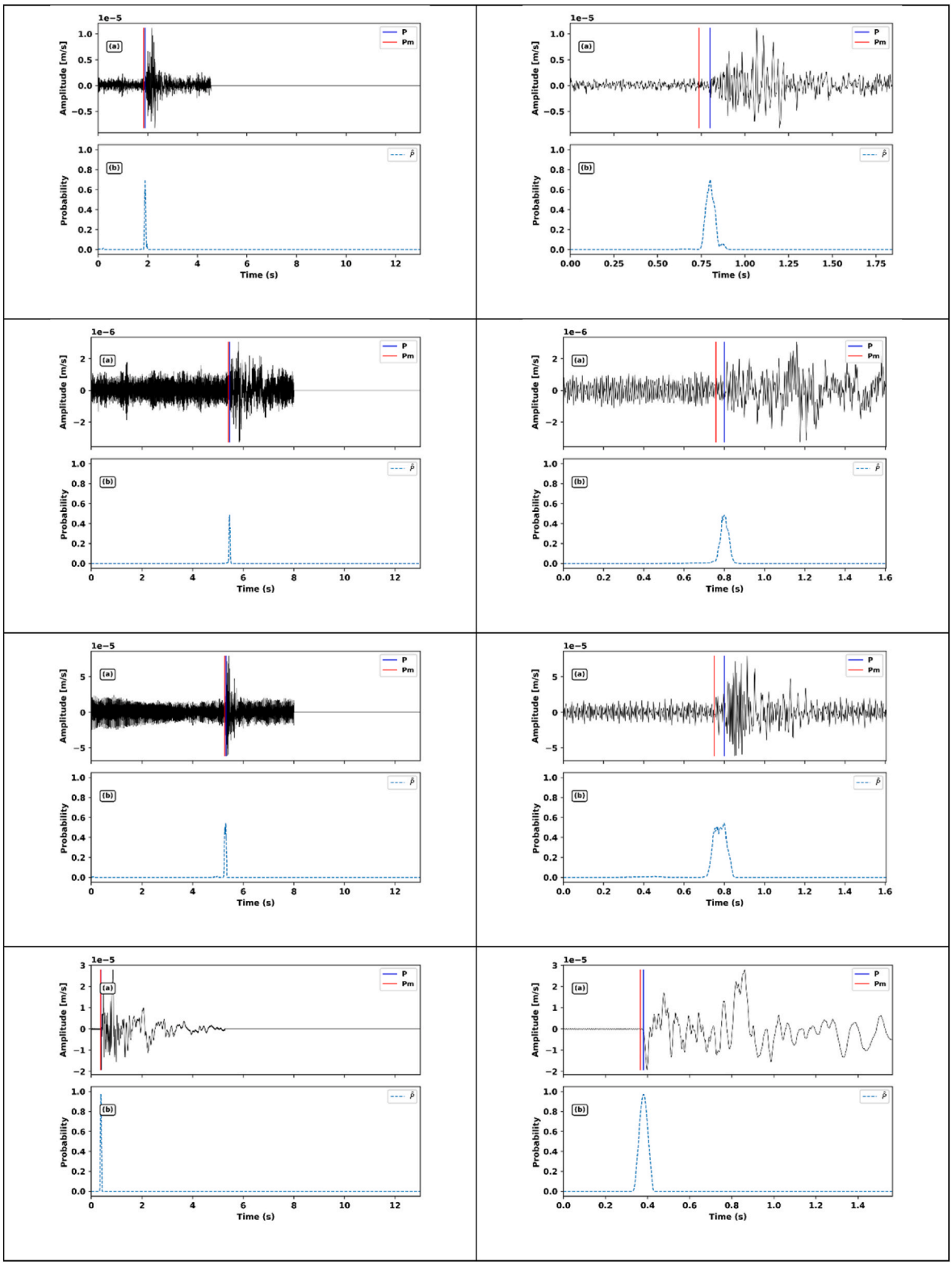

Fig. 6. Examples of picks of seismic P wave onset times in the analyzed data set with small differences between manual picks determined by an expert (Pm) and picks determined by Deep Convolutional Neural Network PhaseNet (P). Left: seismograms shown in a long time window; Right: seismograms shown in a short time window.

showing the huge breakthrough in this research area.

Fig. 5 presents comparison of seismic P wave onset times of the analyzed velocity seismograms from Marcel mine recorded in coal panel C-4/505 determined by an human expert (Pm) and determined by Deep Convolutional Neural Network PhaseNet model with very small differences between them of the order of a few milliseconds. The onset time of the PhaseNet model is determined as the maximum on the presented P wave probability distribution. Fig. 6 depicts the comparison of seismic P wave onset times of the analyzed velocity seismograms determined by a human expert (Pm) and determined by the PhaseNet

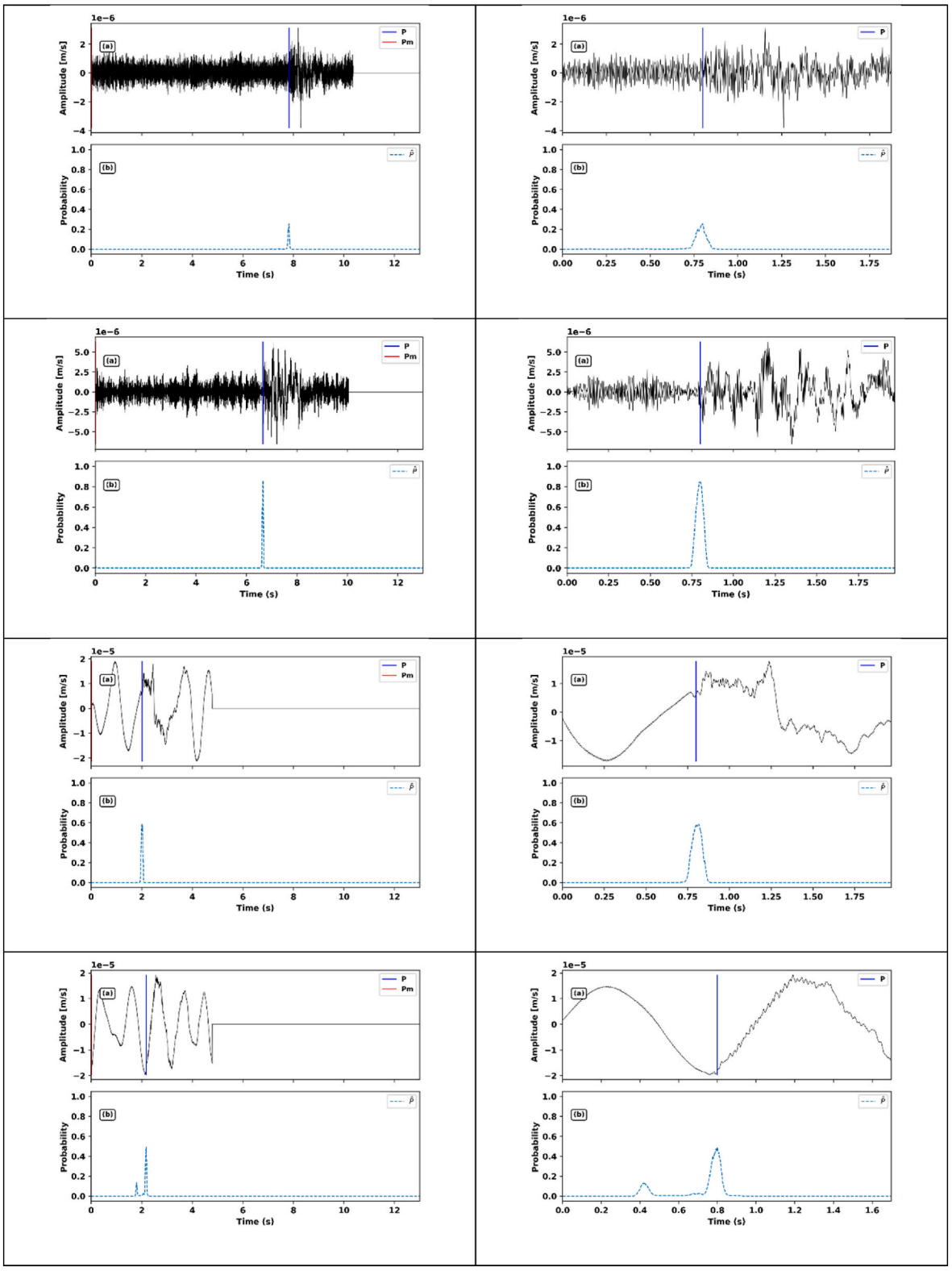

Fig. 7. Examples of picks of seismic P wave onset times in the analyzed data set with high seismic noise and picks determined by Deep Convolutional Neural Network PhaseNet (P) only. Left: seismograms shown in a long time window; Right: seismograms shown in a short time window.

model with differences between them of the order of tens of milliseconds. It is clearly visible that seismic noise of these seismograms is significantly higher and the onset times determined by PhaseNet model are more related to the beginning of the phase of seismic P wave. Likewise, Fig. 7 shows comparison of seismic P wave onset times of the analyzed velocity seismograms determined by PhaseNet model only where human expert was not able to determine the picks. We can easily see that seismic noise of these seismograms is significantly higher than in two previous cases and that the two bottom seismograms in this figure contain slowly varying seismic noise, making it very difficult to analyze

by an expert. However, the PhaseNet model provided reliable results that we verified after more detailed and time-consuming analysis of seismograms.

Overall, the quality of the obtained onset times of seismic P wave utilizing deep neural network PhaseNet model is in most analyzed cases the same or better than human expert. It should be emphasized, however, that the assessment of the quality of determined onset times of seismic P wave is partly subjective, as it was carried out by the authors of this work. Summarizing these results, Fig. 8 shows the distribution of residuals Dt i.e. difference between onset times of seismic P wave determined by Convolutional Deep Neural Network and human expert. Most of the residuals Dt are in the range between −20 and 20 ms confirming indirectly high quality results obtained by PhaseNet model.

All P wave onset times automatically determined by the PhaseNet deep neural network were used to automatically calculate 5544 seismic event locations using formula (1), Fig. 1b, and then to calculate their corresponding seismic energies using formula (2), Fig. 3. Around 10% of the 5544 seismic event locations and seismic energies were calculated with manual picks. It is important to emphasize that a constant velocity model was used for seismic event locations and its approximate nature could lead to source location errors. For this reason, corrections are sometimes made to onset time of seismic P wave to account for these errors. However, this approach hides the fact of heterogeneity in the seismic velocity model and was not considered as a possibility of further tuning the deep neural network to the empirical data.

3.2. Hierarchical spatio-temporal cluster analysis

In the cluster grouping of mining seismicity in Marcel coal mine, we have employed the hierarchical algorithm with a spatio-temporal metric, (Lurka, 2021). However, due to large location errors in the Z coordinate of mining seismic events, the spatio-temporal clustering was conducted using only the horizontal, XY coordinates. Therefore, we have implicitly assumed that all analyzed seismic events are projected onto a horizontal plane at the current mining level. This assumption is acceptable for seismic hazard analysis if coal production is conducted at one horizontal mining level and seismic activity is related to it, Cai et al. (2014).

In the first stage, we have created the dendrogram of spatio-temporal clustering, Fig. 9 what helped us to form group of clusters with similar spatial and temporal coordinates. For our analysis, as a rule of thumb, we made the assumption that the top 20 clusters would be studied and that most of the clusters consist of more than 100 mining tremors, as indicated in Table 1 and Figs. 10–11 so as to obtain a representative sample for statistical calculations.

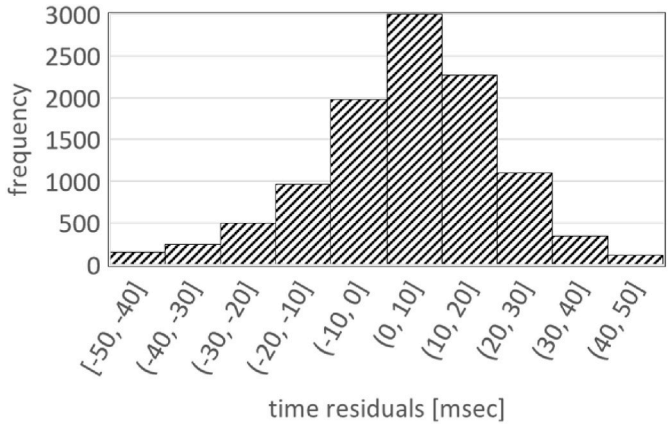

Fig. 8. The distribution of residuals Dt i.e. the difference between phase picks of seismic P wave arrival time determined by the convolutional deep neural network and the human expert of the recorded seismograms for mining seismic events in the Marcel mine.

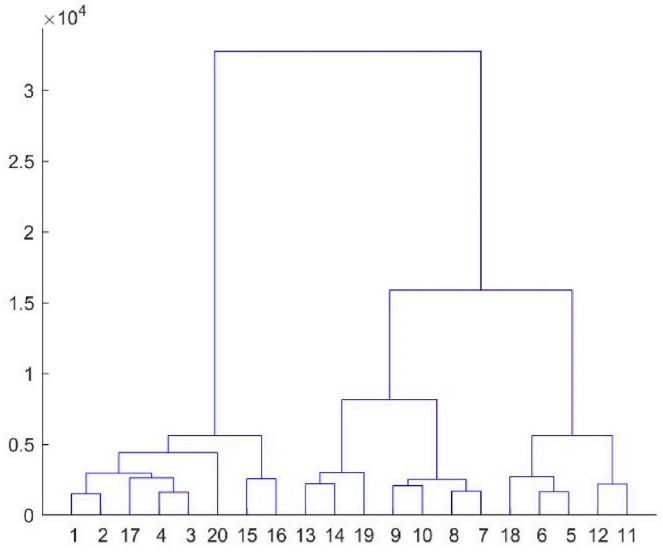

Fig. 9. The dendrogram of the clustering of mining tremors from Marcel mine, Poland. On the horizontal axis, the cluster numbers are displayed, while the vertical axis represents Ward's distance.

The clustering technique generates the succeeding cluster groups based on their spatial and temporal characteristics: (1,2,17,4,3,20,15,16) – group I, (13,14,19) – group II, (9,10,8,7) – group III, (18,6,5,12,11) – group IV, Fig. 9. The rockburst depicted in Fig. 1b is identified as part of Group IV within Cluster 12 through spatio-temporal clustering. The analysis reveals that mining tremors have been successfully separated in terms of spatial and temporal coordinates, as shown in Figs. 10 and 11. This demonstrates the efficacy of our clustering approach resulting in the formation of cohesive clusters for seismic sources generated continuously during longwall mining operations, Fig. 1b and our study presents essential properties of our clustering procedure. These properties include the number of mining tremors, the centroid X, Y and T coordinates representing the spatial and temporal location and the duration of the cluster in days. Furthermore, the distribution of mining tremors depicted in Fig. 10 highlights interrelations among clusters associated with the rockburst: 5 → 6 → 12 → 19 → 7 → 2 → 1.

The term interrelation in our analysis means consecutive occurrence and close proximity in space and time. We have purposely omitted the cluster 11 in this correlation because it has a strong spatial and temporal correlation with cluster 12 and assumed that cluster 11 is part of cluster 12 in our analysis.

3.3. Categorical data analysis

We have started our categorical data analysis by introducing Seismic Energy Levels (SEL) dividing all recorded mining seismic events into 4 categories shown in Table 2. These 4 categories are related to rockburst and seismic hazard due to the simple fact that the more seismic events belong to higher Seismic Energy Level category the higher seismic and rockburst hazard, but this statement is only qualitative and quantitative analysis of this dependence is presented in this paragraph that reveals associations between Seismic Energy Level and Cluster Number categorical variables. Having these energy levels assigned for each analyzed seismic event, we were able to calculate a two way contingency table where the response variable is the cluster number of the performed spatio-temporal clustering and the explanatory variable is Seismic Energy Level. The analyzed contingency table has been presented in Fig. 12 where Seismic Energy Levels were shown in rows and cluster numbers in columns. Each element in the analyzed contingency table is named a cell. Graphical representation of cells in Fig. 12 contains a filled circle

Table 1
The fundamental properties of the clusters obtained through the application of clustering of the mining tremors from Marcel mine, Poland.

Cluster No.	No. of seismic events	Centroid X[m]	Centroid Y[m]	Centroid T[days]	Date START	Date END	DURATION [days]
1	117	43005	25170	783	July 13, 2019	March 13, 2020	244
2	206	42863	25083	756	July 17, 2019	March 09, 2020	236
3	311	42601	25573	240	May 10, 2018	September 04, 2018	116
4	415	42676	25657	237	April 27, 2018	October 15, 2018	171
5	307	42860	25287	357	September 11, 2018	December 15, 2018	95
6	352	42911	25208	412	June 27, 2018	April 01, 2019	278
7	69	43022	25080	649	June 03, 2019	November 02, 2019	152
8	403	42578	25696	192	March 07, 2018	July 13, 2018	128
9	19	42649	25597	842	September 26, 2019	September 29, 2020	369
10	24	42460	25947	539	November 05, 2018	December 22, 2019	412
11	310	42866	25092	546	February 07, 2019	August 31, 2019	205
12	441	42905	25068	454	October 03, 2018	April 15, 2019	195
13	111	42924	25108	1076	June 21, 2020	January 23, 2021	216
14	166	42910	25075	912	February 22, 2020	August 13, 2020	173
15	532	42484	25766	153	January 06, 2018	September 21, 2018	258
16	359	42510	25916	131	November 10, 2017	August 09, 2018	272
17	429	42772	25412	324	June 27, 2018	April 13, 2019	290
18	503	42741	25540	276	June 12, 2018	November 04, 2018	145
19	126	43172	25184	511	September 22, 2018	September 28, 2019	371
20	344	42297	26028	51	November 02, 2017	March 24, 2018	142

whose size reflects magnitude of the frequency (or simply the number of seismic events) of Seismic Energy Level for the specific spatio-temporal cluster of mining induced seismicity. Based on this information, one can easily notice that clusters number: 8, 15, 16, 17 and 18 include the largest number of seismic tremors with VeryHigh category of the Seismic Energy Level, while clusters number 6 and 20 include the largest number of seismic tremors with Low category of Seismic Energy Level.

One of the most important questions related to our contingency table is if it reveals any associations between two analyzed categorical variables i.e. if certain values of Seismic Energy Level variable tend to go with certain values of Cluster Number variable. Additionally we would like to determine how strong the association is, assuming it exists. Therefore, we performed the statistical test of independence of these variables based on formula (5) i.e. we performed statistical chi-squared test of independence with null hypothesis stating that: the two analyzed variables are statistically independent. We obtained the following values of the test: X-squared value equal to 10056, degrees of freedom df = 57 and p-value <2.2e-16. The obtained p-value is very small, which clearly indicates that it is very unlikely that the null hypothesis is true and should be rejected and implies that Seismic Energy Level and Cluster Number are associated. Therefore, we have also calculated two measures of association: contingency coefficient, formula (6), equal to 0.803 and Cramer's V coefficient, formula (7) equal 0.778 showing that the analyzed association is quite strong.

The results above strongly support our assumption on statistical dependence between Seismic Energy Level and Cluster Number, but do not reveal which cells in the analyzed contingency table have the largest influence on the observed association. Therefore we have calculated the standardized residuals of the Pearson chi-squared statistic, formula (8), and obtained a graphical matrix where each cell contains a filled circle whose size reflects magnitude of the standardized residuals for our contingency table, Fig. 13. Basing on this graphical matrix we can infer about the nature of dependence of each specific cell, (Agresti, 2012). The greater the absolute value of the cell's standardized residual, the greater its influence on the dependence between the two categorical variables being analyzed. The rule of thumb indicates that the standardized residuals that exceed 2 or 3 should have a significant influence on the dependence between variables, (Agresti, 2012).

The above analysis allows us to conduct the following reasoning. We have find in the spatio-temporal cluster analysis section that the following clusters were interrelated: 5 → 6 → 12 → 19 → 7 → 2 → 1 where the rockburst was included into the cluster number 12. By comparing the magnitude of standard residuals in the above clusters, it can be noticed that clusters 5 and 6 have had the values greater than 2 in their corresponding cells indicating that they contributed significantly to the dependence between two analyzed categorical variables whereas clusters 19 and 7 contributed very little to this dependence. We can additionally assume that seismic and rockburst hazard was higher before the occurrence of the rockburst i.e. in clusters 5 and 6 and lower after the occurrence of rockburst i.e. in clusters 19 and 7. This suggests that seismic and rockburst hazard is significantly higher in clusters where we observe a strong association between Seismic Energy Level and Cluster Number.

At the end of the analysis performed, it should be emphasized that the specific location of the rockburst did not have a decisive impact on the results obtained. The proposed cluster and categorical data analysis consisted in examining the strength of the association between clusters and seismic energy levels, which is the essence of the proposed methodology for research on seismic and rock bursts hazards.

Finally, it is also necessary to mention the limitations of the methodology introduced and possible further research on this issue. The new computational method that was used to automatically assess rock burst and seismic hazards in the Marcel hard coal mine in Poland should be verified in different geological and technical mining conditions in several other mines. In mines with highly complex geological and mining conditions, the tool may struggle to provide accurate predictions. Variations in rock types, fault lines, and other geological features can introduce challenges that the tool may not fully account for, leading to potential inaccuracies in hazard assessments.

4. Conclusions

PhaseNet is an advanced deep neural network model that determined the onset times of seismic P waves on digital velocity seismograms of mining seismic events in Marcel coal mine better than the human expert. More than one hundred thousand digital velocity seismograms has been processed by PhaseNet model in very short time of the order of couple of minutes. This allows for automatic calculation of seismic parameters characterizing mining seismic tremors such as location and seismic energy.

The combination of spatio-temporal cluster analysis of mining induced seismicity and the categorical data analysis have been introduced to assess seismic and rockburst hazard. These two methods of seismic data analysis have been jointly used in the form of two way contingency tables providing new approach to seismic and rockburst hazard assessment.

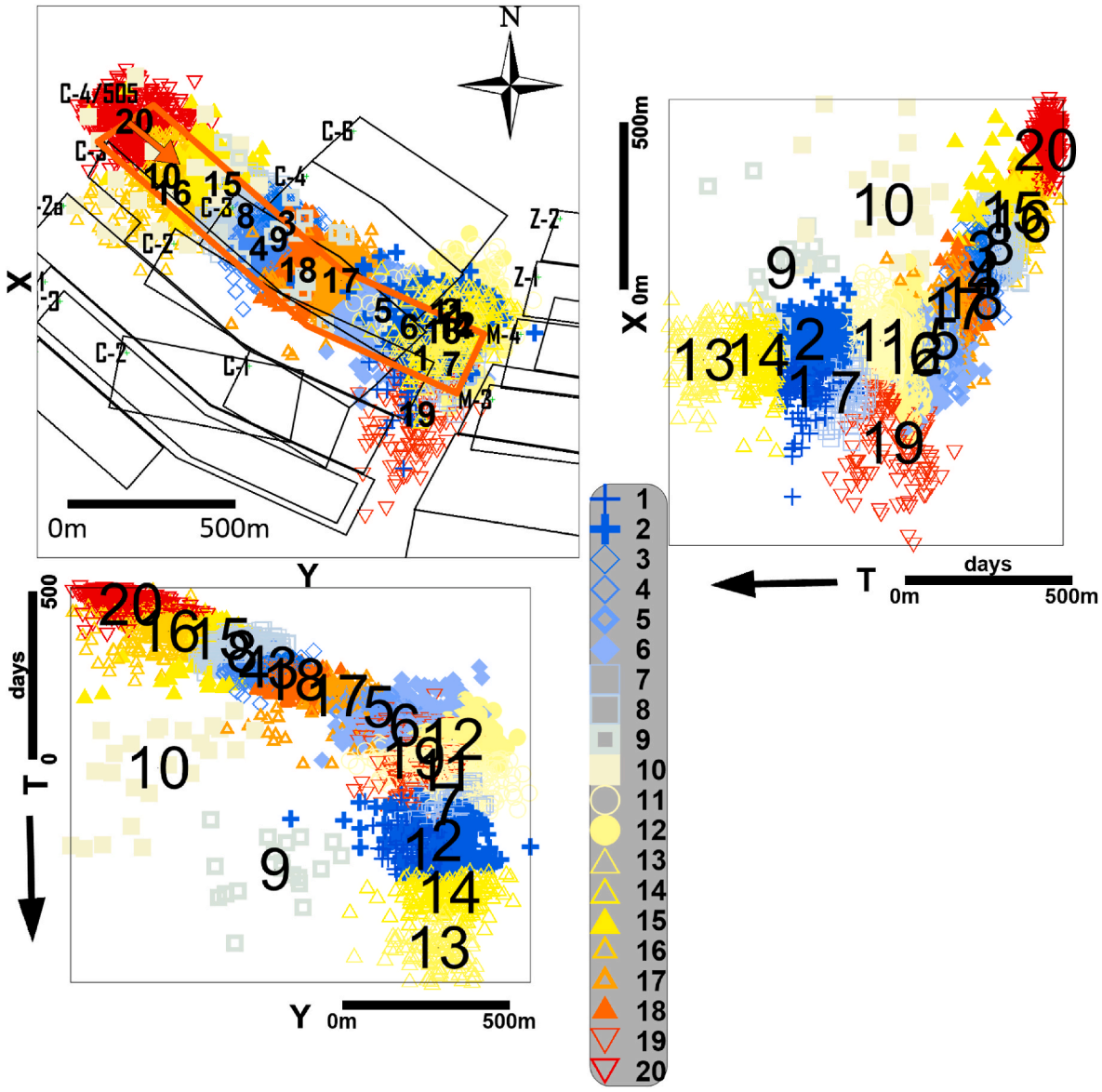

Fig. 10. The outcomes of the clustering of mining tremors from Marcel mine, Poland. The results include the horizontal spatial coordinates (X, Y) and the time coordinate (T) of the mining tremors. Black arrows along T axis indicate time direction.

An automatic computational method that uses the PhaseNet deep neural network model and spatio-temporal clustering has been applied to assess rock burst and seismic hazards in the Marcel hard coal mine in Poland. The seismic and rockburst hazard has been assessed employing two way contingency tables of two categorical variables: Seismic Energy Level of mining tremors and Cluster Number. As a result, a new comprehensive tool has been developed to automatically identify high-stress areas in mines in the form of spatio-temporal clusters.

The practical application of the conducted analysis was demonstrated, yielding valuable insights into the structure of seismicity within each cluster. The examination revealed interrelationships between various analyzed clusters and established a statistical association between the Seismic Energy Level of mining tremors and Cluster Number. A particularly noteworthy statistical association was identified among the clusters located in close proximity to the high-energy seismic event responsible for the rockburst. This observation indicates a strong relationship between the occurrence of the rockburst and the seismic activity in these specific clusters.

The methodology presented, which relies on a deep neural network model, has the potential to become a valuable and routine tool for mining industry in effectively managing seismic risk. Practical implementation for mining industry require to integrate this tool into existing seismic monitoring systems. By incorporating this approach into their practices, mining engineers can enhance their ability to assess and mitigate the potential hazards associated with seismic activity, ultimately improving overall safety and risk management in mining operations.

Authorship statement

Adam Lurka carried out this study and wrote the paper.

Computer code availability

I

Automatic determination of seismic P wave picks were obtained using PhaseNet: A Deep-Neural-Network-Based Seismic Arrival Time Picking Method, code available at https://github.com/AI4EPS/PhaseNet

II

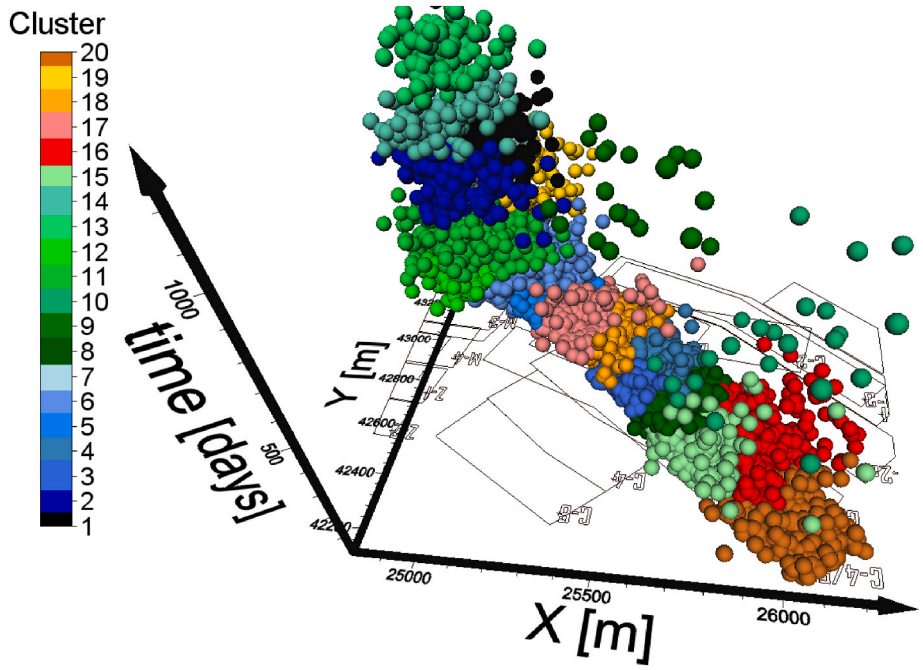

Fig. 11. 3D image of the clustering results of mining tremors from Marcel mine, Poland. The results include the horizontal spatial coordinates (X, Y) and the time coordinate (T) of the mining tremors.

Table 2
Relation between seismic energy levels and seismic energy values of recorded mining seismic events in the Marcel mine.

Seismic Energy Level	Seismic Energy Range [J]
Low	$<10^3$
Medium	$\geq 10^3$ and $<10^4$
High	$\geq 10^4$ and $<10^5$
VeryHigh	$\geq 10^5$

Name of the code/library: ClusterContingencyTables
Contact: alurka@gig.eu
Hardware requirements: Windows
Program languages: MatLab, R
Software required: MatLab 2018a, RStudio
The source codes are available for downloading at the link: https://github.com/Quarkal/ClusterContingencyTables

Data availability statement

The authors do not have permission to share data.

Funding

Part of this research was carried out within the project EPOS-PL PLUS, European Plate Observing System POIR.04.02.00–00-C005/19, funded by the Operational Programme Smart Growth 2014–2020, Priority IV: Increasing the research potential, Action 4.2: Development of modern research infrastructure of the science sector, and co-financed from European Regional Development Fund.

CRediT authorship contribution statement

Adam Lurka: Conceptualization, Data curation, Formal analysis, Funding acquisition, Investigation, Methodology, Project administration, Resources, Software, Supervision, Validation, Visualization, Writing – original draft, Writing – review & editing.

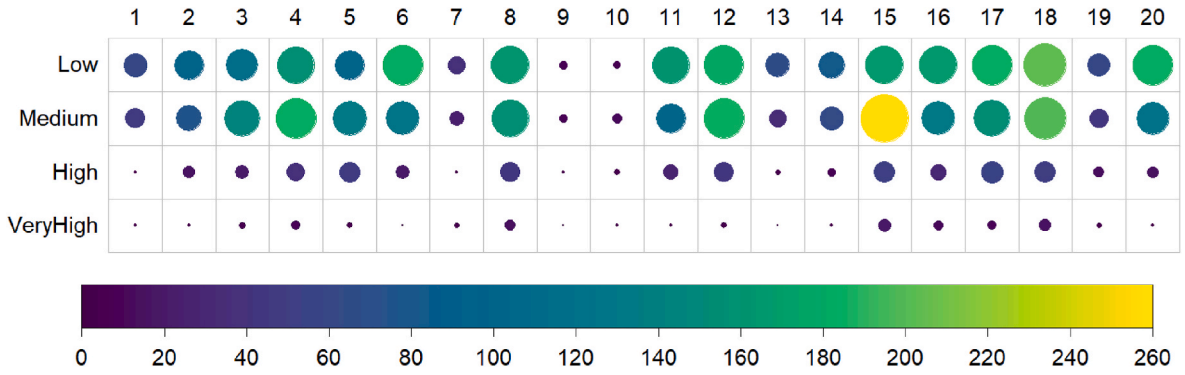

Fig. 12. Graphical matrix representing contingency table of two categorical variables: Cluster Number and Seismic Energy Level. Each cell contains a filled circle whose size reflects magnitude of the frequency of Seismic Energy Level in each cluster.

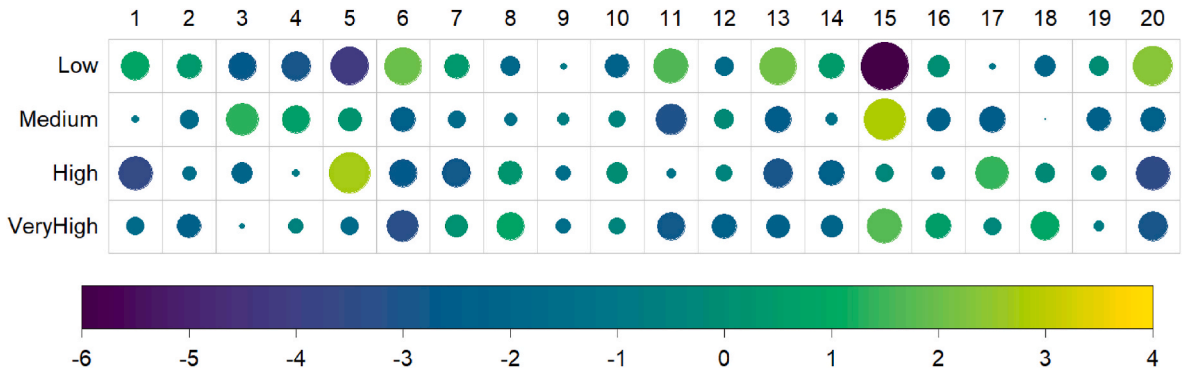

Fig. 13. Graphical matrix where each cell contains a filled circle whose size reflects the magnitude of the standardized residuals for contingency table from Fig. 11 and Fig. 12.

Declaration of competing interest

The authors declare that they have no known competing financial interests or personal relationships that could have appeared to influence the work reported in this paper.

Data availability

Data will be made available on request.

References

Aggarwal, C.C., Reddy, C.K., 2014. Data Clustering in Algorithms and Applications. CRC Press, Boca Raton.

Agresti, A., 2012. Categorical Data Analysis. John Wiley & Sons.

An, Y., Guo, J., Ye, Q., Childs, C., Walsh, J., Dong, R., 2021. Deep convolutional neural network for automatic fault recognition from 3D seismic datasets. Comput. Geosci. 153, 104776 https://doi.org/https://doi.org/10.1016/j.cageo.2021.104776.

Bai, J., Dou, L., Cai, W., Gong, S., Shen, W., Tian, X., Ma, H., 2022. An integration method of bursting strain energy and seismic velocity tomography for coal burst hazard assessment. Lithosphere. https://doi.org/10.2113/2022/2070540, 2022.

Cai, W., Dou, L., Cao, A., Gong, S., Li, Z., 2014. Application of seismic velocity tomography in underground coal mines: a case study of Yima mining area, Henan, China. J. Appl. Geophys. 109 https://doi.org/10.1016/j.jappgeo.2014.07.021.

Cai, W., Dou, L., Si, G., Cao, A., Gong, S., Wang, G., Yuan, S., 2019. A new seismic-based strain energy methodology for coal burst forecasting in underground coal mines. Int. J. Rock Mech. Min. Sci. 123 https://doi.org/10.1016/j.ijrmms.2019.104086.

Cao, W., Durucan, S., Cai, W., Shi, J.Q., Korre, A., Jamnikar, S., Rošer, J., Lurka, A., Siata, R., 2020. The role of mining intensity and pre-existing fracture attributes on spatial, temporal and magnitude characteristics of microseismicity in longwall coal mining. Rock Mech. Rock Eng. https://doi.org/10.1007/s00603-020-02158-4.

Chai, C., Maceira, M., Santos-Villalobos, H., Venkatakrishnan, S., Schoenball, M., Weiqiang, Z., Beroza, G., Thurber, C., Team, E.G.S., 2020. Using a deep neural network and transfer learning to bridge scales for seismic phase picking. Geophys. Res. Lett. 47, e2020GL088651 https://doi.org/10.1029/2020GL088651.

Ding, Z.W., Li, X.F., Huang, X., Wang, M.B., Tang, Q.B., Jia, J.D., 2022. Feature extraction, recognition, and classification of acoustic emission waveform signal of coal rock sample under uniaxial compression. Int. J. Rock Mech. Min. Sci. 160, 105262 https://doi.org/https://doi.org/10.1016/j.ijrmms.2022.105262.

Duan, Y., Shen, Y., Canbulat, I., Luo, X., Si, G., 2021. Classification of clustered microseismic events in a coal mine using machine learning. J. Rock Mech. Geotech. Eng. 13 (6), 1256–1273. https://doi.org/10.1016/j.jrmge.2021.09.002.

Geng, Y., Su, L., Jia, Y., Han, C., 2019. Seismic events prediction using deep temporal convolution networks. Journal of Electrical and Computer Engineering 2019, 7343784. https://doi.org/10.1155/2019/7343784.

Gong, S., Li, J., Ju, F., Dou, L., He, J., Tian, X., 2019. Passive seismic tomography for rockburst risk identification based on adaptive-grid method. Tunn. Undergr. Space Technol. 86, 198–208. https://doi.org/10.1016/j.tust.2019.01.001.

He, M., Zhang, Z., Ren, J., Huan, J., Li, G., Chen, Y., Li, N., 2019. Deep convolutional neural network for fast determination of the rock strength parameters using drilling data. Int. J. Rock Mech. Min. Sci. 123, 104084 https://doi.org/https://doi.org/10.1016/j.ijrmms.2019.104084.

Hudyma, M., 2008. Analysis and Interpretation of Clusters of Seismic Events in Mines. University of Western Australia. PhD thesis.

Jain, A.K., Murty, M.N., Flynn, P.J., 1999. Data clustering: a review. ACM Comput. Surv. 31 (3), 264–323 http://doi.acm.org/10.1145/331499.331504.

Johnson, S.W., Chambers, D.J.A., Boltz, M.S., Koper, K.D., 2021. Application of a convolutional neural network for seismic phase picking of mining-induced seismicity. Geophys. J. Int. 224 (1), 230–240. https://doi.org/10.1093/gji/ggaa449.

Kanamori, H., Mori, J., Hauksson, E., Heaton, T.H., Hutton, L.K., Jones, L.M., 1993. Determination of earthquake energy release and ML using TERRAscope. Bull. Seismol. Soc. Am. 83 (2), 330–346. https://doi.org/10.1785/BSSA0830020330.

Kwiatek, G., Plenkers, K., Nakatani, M., Yabe, Y., Dresen, G., JAGUARS-Group, 2010. Frequency-magnitude characteristics down to magnitude -4.4 for induced seismicity recorded at mponeng gold mine, South Africa. Bull. Seismol. Soc. Am. 100, 1165–1173. https://doi.org/10.1785/0120090277.

Leśniak, A., Isakow, Z., 2009. Space–time clustering of seismic events and hazard assessment in the Zabrze-Bielszowice coal mine, Poland. Int. J. Rock Mech. Min. Sci. 46, 918–928. https://doi.org/10.1016/j.ijrmms.2008.12.003.

Liu, C., Chen, Q., 2023a. Deep learning-based multi-parameter early warning model under true triaxial conditions. Eng. Geol. 319, 107111 https://doi.org/https://doi.org/10.1016/j.enggeo.2023.107111.

Liu, C., Chen, Q., 2023b. Deep learning-based multi-parameter early warning model under true triaxial conditions. Eng. Geol. 319, 107111 https://doi.org/https://doi.org/10.1016/j.enggeo.2023.107111.

Liu, Y., Cao, A., Wang, C., Yang, X., Wang, Q., Bai, X., 2023. Cluster analysis of moment tensor solutions and its application to rockburst risk assessment in underground coal mines. Rock Mech. Rock Eng. https://doi.org/10.1007/s00603-023-03388-y.

Lurka, A., 2021. Spatio-temporal hierarchical cluster analysis of mining-induced seismicity in coal mines using Ward's minimum variance method. J. Appl. Geophys. 184, 104249 https://doi.org/https://doi.org/10.1016/j.jappgeo.2020.104249.

Ma, K., Sun, X., Zhang, Z., Hu, J., Wang, Z., 2022. Intelligent location of microseismic events based on a fully convolutional neural network (FCNN). Rock Mech. Rock Eng. 55 (8), 4801–4817. https://doi.org/10.1007/s00603-022-02911-x.

Mao, H., Xu, N., Li, X., Li, B., Xiao, P., Li, Y., Li, P., 2023. Analysis of rockburst mechanism and warning based on microseismic moment tensors and dynamic Bayesian networks. J. Rock Mech. Geotech. Eng. https://doi.org/https://doi.org/10.1016/j.jrmge.2022.12.005.

Meyer, S., Bassom, A., Reading, A., 2019. Delineation of fault segments in mines using seismic source mechanisms and location uncertainty. J. Appl. Geophys. 170, 103828 https://doi.org/10.1016/j.jappgeo.2019.103828.

Mousavi, S.M., Ellsworth, W.L., Zhu, W., Chuang, L.Y., Beroza, G.C., 2020. Earthquake transformer—an attentive deep-learning model for simultaneous earthquake detection and phase picking. Nat. Commun. 11 (1), 3952. https://doi.org/10.1038/s41467-020-17591-w.

Mutke, G., Dubiński, J., Lurka, A., 2015. New Criteria to Assess Seismic and Rock Burst Hazard in Coal Mines/Nowe Kryteria Dla Oceny Zagrożenia Sejsmicznego I Tąpaniami W Kopalniach Węgla Kamiennego. Archives of Mining Sciences. https://doi.org/10.1515/amsc-2015-0049.

Niu, W., Feng, X.-T., Yao, Z., Bi, X., Yang, C., Hu, L., Zhang, W., 2022. Types and occurrence time of rockbursts in tunnel affected by geological conditions and drilling & blasting procedures. Eng. Geol. 303, 106671 https://doi.org/https://doi.org/10.1016/j.enggeo.2022.106671.

Orlecka-Sikora, B., Lasocki, S., Lizurek, G., Rudziński, Ł., 2012. Response of seismic activity in mines to the stress changes due to mining induced strong seismic events. Int. J. Rock Mech. Min. Sci. 53, 151–158. https://doi.org/10.1016/j.ijrmms.2012.05.010, 2012.

Press, W.H., Teukolsky, S.A., Vetterling, W.T., Flannery, B.P., 2007. Numerical Recipes 3rd Edition: the Art of Scientific Computing. Cambridge University Press, Cambridge.

Prugger, A., Gendzwill, D., 1988. Microearthquake location: a nonlinear approach that makes use of a simplex stepping procedure. Bull. Seismol. Soc. Am. 78, 799–815. https://doi.org/10.1785/BSSA0780020799.

Pu, Y., Apel, D.B., Hall, R., 2020. Using machine learning approach for microseismic events recognition in underground excavations: comparison of ten frequently-used models. Eng. Geol. 268, 105519 https://doi.org/https://doi.org/10.1016/j.enggeo.2020.105519.

Pu, Y., Chen, J., Jiang, D., Apel, D.B., 2022. Improved method for acoustic emission source location in rocks without prior information. Rock Mech. Rock Eng. 55 (8), 5123–5137. https://doi.org/10.1007/s00603-022-02909-5.

Riemer, K.L., Durrheim, R.J., 2012. Mining seismicity in the Witwatersrand Basin: monitoring, mechanisms and mitigation strategies in perspective. J. Rock Mech.

Geotech. Eng. 4 (3), 228–249 https://doi.org/https://doi.org/10.3724/SP.J.1235.2012.00228.
Ronneberger, O., Fischer, P., Brox, T., 2015. U-net: convolutional networks for biomedical image segmentation. LNCS 9351. https://doi.org/10.1007/978-3-319-24574-4_28.
Ross, Z.E., Meier, M., Hauksson, E., Heaton, T.H., 2018. Generalized seismic phase detection with deep learning. Bull. Seismol. Soc. Am. 108 (5A), 2894–2901. https://doi.org/10.1785/0120180080.
Shuai, C., Dou, L., Zhang, L., Song, J., Xu, J., Han, Z., 2023. Mechanism of reducing the bursting liability of coal using liquid nitrogen cyclic fracturing. Nat. Resour. Res. https://doi.org/10.1007/s11053-023-10191-7.
Sun, H., Liu, X.L., Zhu, J.B., 2019. Correlational fractal characterisation of stress and acoustic emission during coal and rock failure under multilevel dynamic loading. Int. J. Rock Mech. Min. Sci. 117, 1–10 https://doi.org/https://doi.org/10.1016/j.ijrmms.2019.03.002.
Thurber, C.H., Engdahl, E.R., 2000. Advances in global seismic event location. In: Thurber, C.H., Rabinowitz, N. (Eds.), Advances in Seismic Event Location. Modern Approaches in Geophysics, 18. Springer, Dordrecht. https://doi.org/10.1007/978-94-015-9536-0_1.
Wang, G. feng, Gong, S. yuan, Dou, L. ming, Cai, W., Jin, F., Fan, C. jun, 2019. Behaviour and bursting failure of roadways based on a pendulum impact test facility. Tunn. Undergr. Space Technol. 92 https://doi.org/10.1016/j.tust.2019.103042.
Wang, G., Gong, S., Li, Z., Dou, L., Cai, W., Mao, Y., 2015. Evolution of stress concentration and energy release before rock bursts: two case studies from xingan coal mine, hegang, China. Rock Mech. Rock Eng. 49 https://doi.org/10.1007/s00603-015-0892-x.
Wang, J.X., Tang, S.B., Heap, M.J., Tang, C.A., Tang, L.X., 2021. An auto-detection network to provide an automated real-time early warning of rock engineering hazards using microseismic monitoring. Int. J. Rock Mech. Min. Sci. 140, 104685 https://doi.org/https://doi.org/10.1016/j.ijrmms.2021.104685.
Wang, J., Tang, S., 2022. Novel transfer learning framework for microseismic event recognition between multiple monitoring projects. Rock Mech. Rock Eng. 55 (6), 3563–3582. https://doi.org/10.1007/s00603-022-02790-2.
Wang, J., Xiao, Z., Liu, C., Zhao, D., Yao, Z., 2019. Deep learning for picking seismic arrival times. J. Geophys. Res. Solid Earth 124 (7), 6612–6624. https://doi.org/10.1029/2019JB017536.
Wilkins, A.H., Strange, A., Duan, Y., Luo, X., 2020. Identifying microseismic events in a mining scenario using a convolutional neural network. Comput. Geosci. 137, 104418 https://doi.org/https://doi.org/10.1016/j.cageo.2020.104418.
Woodward, K., Wesseloo, J., Potvin, Y., 2018. A spatially focused clustering methodology for mining seismicity. Eng. Geol. 232, 104–113. https://doi.org/10.1016/j.enggeo.2017.11.015.
Woollam, J., Münchmeyer, J., Tilmann, F., Rietbrock, A., Lange, D., Bornstein, T., Diehl, T., Giunchi, C., Haslinger, F., Jozinović, D., Michelini, A., Saul, J., Soto, H., 2022. SeisBench—a toolbox for machine learning in seismology. Seismol Res. Lett. 93 (3), 1695–1709. https://doi.org/10.1785/0220210324.
Xu, H., Zhao, Y., Yang, T., Wang, S., Chang, Y., Jia, P., 2022. An automatic P-wave onset time picking method for mining-induced microseismic data based on long short-term memory deep neural network. Geomatics, Nat. Hazards Risk 13 (1), 908–933. https://doi.org/10.1080/19475705.2022.2057241.
Xu, R., Puzyrev, V., Elders, C., Fathi Salmi, E., Sellers, E., 2023. Deep semi-supervised learning using generative adversarial networks for automated seismic facies classification of mass transport complex. Comput. Geosci. 180, 105450 https://doi.org/https://doi.org/10.1016/j.cageo.2023.105450.
Zhang, W., Phoon, K.K., 2022. Editorial for Advances and applications of deep learning and soft computing in geotechnical underground engineering. J. Rock Mech. Geotech. Eng. 14 (3), 671–673. https://doi.org/10.1016/j.jrmge.2022.01.001. Chinese Academy of Sciences.
Zhou, X., Ouyang, Z., Zhou, R., Ji, Z., Yi, H., Tang, Z., Chang, B., Yang, C., Sun, B., 2021. An approach to dynamic disaster prevention in strong rock burst coal seam under multi-aquifers: a case study of tingnan coal mine. Energies 14, 7287. https://doi.org/10.3390/en14217287.
Zhu, G., Dou, L., Wang, C., Ding, Z., Feng, Z., Xue, F., 2019. Experimental study of rock burst in coal samples under overstress and true-triaxial unloading through passive velocity tomography. Saf. Sci. 117, 388–403. https://doi.org/10.1016/j.ssci.2019.04.012.
Zhu, M., Cheng, J., Zhang, Z., 2021. Quality control of microseismic P-phase arrival picks in coal mine based on machine learning. Comput. Geosci. 156, 104862 https://doi.org/https://doi.org/10.1016/j.cageo.2021.104862.
Zhu, W., Beroza, G.C., 2019. PhaseNet: a deep-neural-network-based seismic arrival-time picking method. Geophys. J. Int. 216 (1), 261–273. https://doi.org/10.1093/gji/ggy423.
Zou, G., Liu, H., Ren, K., Deng, B., Xue, 2022. J. Automatic recognition of faults in mining areas based on convolutional neural network. Energies 15, 3758. https://doi.org/10.3390/en15103758.